Arman Kheirati Roonizi

# Fourier Analysis

*A new computing approach*

Fourier expansion is a special case of signal decomposition that decomposes a signal into oscillatory components. In this method, the signal is represented as a linear combination of trigonometric or exponential basis functions. The expansion coefficients (or weights) are then computed by correlating the signal with the corresponding basis functions [1], [2]. The process of computing the coefficients is known as *Fourier analysis*. In real applications, we are interested in using a few terms of a Fourier expansion, or it may be impossible to use all of the terms to approximate the signal. Therefore, a truncated Fourier expansion is used instead [3]. However, when a truncated Fourier expansion is used to approximate a signal with a jump discontinuity, an overshoot/undershoot at the discontinuity occurs, which is known as the *Gibbs phenomenon*. The correct size of the overshoot and the undershoot of a truncated Fourier expansion near the point of discontinuity was computed by Gibbs; the size of the overshoot/undershoot is approximately 9% of the magnitude of the jump [4].

This article demonstrates that the size of the overshoot depends mainly on the approach used for computing the Fourier analysis. It shows that, in the traditional approach, the Fourier analysis is computed based on the

minimization of the mean square error (MSE) between the signal and its Fourier expansion (i.e., the $\ell_2$-norm minimization of the model error). Then it presents a new method to compute the Fourier analysis. In the new approach, the Fourier analysis (expansion coefficients) is obtained by minimizing the mean absolute error (MAE) between the reconstructed signal and the original signal. Since the new approach is defined based on the $\ell_1$-norm minimization, we call it $\ell_1$ Fourier analysis. Similarly, the traditional approach is called $\ell_2$ Fourier analysis.

Using $\ell_1$ Fourier analysis, we observed that the size of the overshoot/undershoot for a truncated Fourier expansion of signals with jump discontinuities is decreased to 4% of the magnitude of the jump. The effectiveness of the proposed $\ell_1$ Fourier analysis, in terms of reduction of the Gibbs phenomenon in a truncated Fourier series expansion and filtering of the impulsive noise from the signals and images, is showcased using numerical examples.

## Relevance

In signal analysis, one often encounters Fourier analysis. It is one of the most important tools in mathematics, computer science, and signal processing and is used where one needs to solve a partial differential equation [5], compress music in MP3 players [6], compress digital images in JPEG form [7], or perform digital spectral analysis

[8] and filter design [9], to name just a few applications. The method consists of two steps: 1) decomposing the signal into oscillatory components by expanding it based on a linear combination of a set of trigonometric or exponential functions with fundamental frequencies and 2) computing the Fourier analysis or finding the expansion coefficients. It was first introduced by Baron Jean Baptiste Joseph Fourier in 1807 to derive equations of heat propagation using some series of trigonometric functions [10]. The original derivation by Fourier was proposed for representing a continuous-time (CT) signal. Today, because of the power of digital computers, Fourier analysis is mainly presented in the context of discrete-time signals (sequences) and systems. The most important transform that performs Fourier analysis for discrete signals is the discrete Fourier transform (DFT). The formulations of discrete Fourier analysis (or the DFT) and their CT counterparts (continuous Fourier series) are quite similar with some differences. In 1965, Cooley and Tukey jointly developed an implementation of DFT for high-speed computers, which is known as the *fast Fourier transform* [11].

In this article, we concern ourselves mainly with the DFT, which is of great practical importance in the analysis of discrete signals and other data. We study the Gibbs phenomenon in truncated Fourier expansions of functions with jump discontinuities

and propose a new approach to compute a DFT (Fourier coefficients) that reduces the Gibbs effect. The method is based on the replacement of an $\ell_2$-norm with an $\ell_1$-norm. It minimizes the MAE between the signal and its Fourier expansion. The replacement of the $\ell_2$-norm with the $\ell_1$-norm is a treatment that has been studied for two decades in sparse solutions [12], [13] and compressed sensing [14]. Especially in many applications in compressed sensing, the measurement matrix is a Fourier matrix [15]. Compressive sensing shows that a compressed signal can be reconstructed from much fewer incoherent measurements. Its aim is to represent a sparse signal without going through the intermediate stage of acquiring all of the samples. It is also related to the problem of reconstructing a signal from incomplete frequency information [16].

The $\ell_1$-norm has also been attracting an increasing amount of attention for the interpolation and approximation of functions and irregular geometric data. In [17], the authors show that the Gibbs phenomenon can be reduced by using $\ell_1$ spline fits. In [18], some theoretical results are provided to explain the potential of such methods in avoiding Gibbs phenomena. While none of the previous algorithms uses the $\ell_1$-norm to identify the expansion coefficients, in this article, the process of computing the Fourier analysis is defined based on the $\ell_1$-norm minimization of the error between the reconstructed signal and the original signal. The main problem is that there is no analytic formula for its solution. Therefore, a majorization–minimization (MM) approach [19] is used to solve the problem, which results in a linear iterative algorithm.

## Prerequisites

This article requires a basic knowledge of signals and systems, engineering mathematics, and optimization problems.

## The DFT

The inverse DFT states that a discrete signal can be represented as a linear combination of trigonometric/exponential functions with fundamental frequencies. That is, a given signal $x[n]$, $n \in \mathbb{Z}_N = \{0, 1, \ldots, N-1\}$ can be represented as [9], [20]

$$x[n] = \sum_{k=0}^{N-1} c_k e^{i\frac{2\pi k}{N}n}, \qquad (1)$$

where $i = \sqrt{-1}$, and the expansion coefficients $c_k$ are given by

$$c_k = \frac{1}{N}\sum_{n=0}^{N-1} x[n] e^{-i\frac{2\pi k}{N}n}. \qquad (2)$$

Some authors include the factor $1/N$ in the definition of $x[n]$ and not in the definition of Fourier analysis [21], [22], [23]. Equation (2) is simply obtained by multiplying both sides of (1) by $e^{i(2\pi j/N)n}$, taking the sum of the result from 0 to $N-1$, and simplifying it while considering the following relation:

$$\frac{1}{N}\sum_{n=0}^{N-1} e^{i\frac{2\pi j}{N}n} e^{i\frac{2\pi k}{N}n} = \begin{cases} 0 & \text{if } j \neq k \\ 1 & \text{if } j = k \end{cases}. \qquad (3)$$

Note that when $x$ is real valued, its Fourier expansion is usually written in terms of sines and cosines:

$$x[n] = \sum_{k=0}^{N-1} \alpha_k \cos\left(\frac{2\pi k}{N}n\right) + \beta_k \sin\left(\frac{2\pi k}{N}n\right), \qquad (4)$$

where the coefficients $\alpha_k$ and $\beta_k$ are computed as

$$\begin{cases} \alpha_k = \frac{1}{N}\sum_{n=0}^{N-1} x[n]\cos\left(\frac{2\pi k}{N}n\right) \\ \beta_k = \frac{1}{N}\sum_{n=0}^{N-1} x[n]\sin\left(\frac{2\pi k}{N}n\right) \end{cases}. \qquad (5)$$

Note that $c_k$, $\alpha_k$, and $\beta_k$ are related as $c_k = (\alpha_k - i\beta_k)/2$. In real applications, we are interested in using a few terms of a Fourier expansion, or it may be impossible to use all of the terms to approximate the signal. Therefore, a truncated Fourier expansion is used instead. In the following section, the problem of representing the signals with a truncated Fourier expansion and its limitations are discussed.

## Problem statement

Let us consider the problem of approximating $x[n]$ by a truncated Fourier expansion $x_M[n]$, defined by

$$x_M[n] = \sum_{k=0}^{M-1} c_k e^{i\frac{2\pi k}{N}n}, \quad M < N. \quad (6)$$

In a truncated Fourier expansion, the number of expansion terms is less than the length of the signal. When (6) is used to approximate a signal with a jump discontinuity, an overshoot at the discontinuity occurs. This phenomenon was observed by Michelson when he was using his mechanical machine (called a *harmonic analyzer*) to produce graphs of truncated trigonometric series with terms of up to 80 sines and cosines. He published his report [24], and the problem was explained by Gibbs [25], [26] in 1899; thus it is known as the Gibbs phenomenon. However, the history of studying the overshoot and undershoot in the neighborhood of discontinuities of the sums of Fourier series goes back to 1848, when Wilbraham published an article on this topic for the first time [27]. The Gibbs effect is also seen in other signal decomposition approaches, such as wavelet expansion and spline and cubic spline interpolation [17], [18], [28].

As an illustration of the Gibbs phenomenon, we consider a step function with 10 s duration sampled at 0.0098 s (i.e., $N = 1,024$) and its Fourier expansion using the truncated model (6). The step function and its truncated Fourier expansion with the first $M$ modes, i.e., $x_M[n]$, for $M = 8, 32, 64$, and 128, are shown via the blue and red lines in Figure 1. The first plot includes only the first eight modes in the Fourier expansion, while the last plot includes up to 128 modes. The more modes we include, the more the curve looks like a step function. However, it introduces strange wiggles (overshoots) near the discontinuity. As the number of modes grows, the wiggles are pushed increasingly closer to the discontinuity, in the sense that the amplitude in a given region decreases as the number of modes, $M$, increases. So, in some sense, the wiggles go away as $M$ approaches $N$. However, the overshoot unfortunately never goes away, but it remains roughly the same size (about 9% of the magnitude of the jump). It is provable that this 9% result holds for a discontinuity in any function, not just a step function [4]. So, the question arises as to whether this 9% overshoot is due to the Fourier expansion or to the approach used for computing the

expansion coefficients. If it is the latter case, is it possible to decrease the Gibbs effect by employing a different computation approach? This article shows that the 9% overshoot of the Fourier expansion reported in the literature is due to the approach used for computing the Fourier analysis, and it can be decreased if we employ the proper approach to compute the coefficients.

## Solution

As will become clear in the following discussion, the Fourier analysis (expansion coefficients) computed by (2) minimizes the MSE between the signal and its Fourier expansion. The MSE corresponds to the $\ell_2$-norm. It also gives the maximum likelihood (ML) estimate of the coefficients, under the assumption of a white Gaussian distribution for the modeling error. The problem is that this assumption does not hold in practice. Specifically, for the previous example, the estimation error confirms a non-Gaussian distribution. We will see that, for the truncated Fourier expansion of the step function, the Gibbs phenomenon can be reduced if the Fourier coefficients are computed by minimizing the MAE between the signal and its model.

### MSE-based Fourier analysis computation

Equation (6) can be written in the following form:

$$x_M[n] = \sum_{k=0}^{M-1} c_k \phi_k[n], \qquad (7)$$

where

$$\phi_k[n] = e^{i\frac{2\pi k}{N}n}. \qquad (8)$$

The expansion error is defined by $e[n] = x[n] - x_M[n]$, i.e.,

$$e[n] = x[n] - \sum_{k=0}^{M-1} c_k \phi_k[n].$$

An important property for the expansion model is its ability in signal approximation; that is, the error signal should be within an acceptable range. Let us consider that the parameters are found by minimizing the power of the residual error signal, $e[n]$:

$$\hat{c}_k = \operatorname*{argmin}_{c_k} \frac{1}{N} \sum_{n=0}^{N-1} \left( x[n] - \sum_{k=0}^{M-1} c_k \phi_k[n] \right)^2. \qquad (9)$$

Then the minimization of (9) with respect to the coefficients $c_k$ leads to the following solution:

$$\mathbf{c_{opt}} = \mathbf{\Phi}^{-1}\mathbf{x} \qquad (10)$$

where $\mathbf{\Phi} \in \mathbb{R}^{M \times M}$ and $\mathbf{x} \in \mathbb{R}^M$ are, respectively, matrices and vectors with the following entries:

$$\mathbf{\Phi}_{p,q} = \frac{1}{N} \sum_{n=0}^{N-1} \phi_p[n] \phi_q^*[n],$$
$$(p, q = 0, \ldots, M-1)$$

$$\mathbf{x}_q = \frac{1}{N} \sum_{n=0}^{N-1} x[n] \phi_q^*[n]. \qquad (11)$$

Since the Fourier basis functions $\phi_k[n]$ form an orthonormal basis, the matrix $\mathbf{\Phi}$ becomes an identity matrix, and the coefficients are found as

$$\mathbf{c_{opt}} = \mathbf{x}, \qquad (12)$$

which is exactly the same as (2) when we set $M = N$. This means that the Fourier analysis obtained by (2) minimizes the MSE between the signal and its expansion (i.e., the $\ell_2$-norm of the error). Note that (10) is also the ML estimate of the coefficient vector $\mathbf{c}$, under the assumption of a white Gaussian distribution for the modeling error $e[n]$. In the following, we compute the Fourier analysis by minimizing the MAE between the signal and its Fourier expansion (i.e., the $\ell_1$-norm minimization of the error).

### MAE-based Fourier analysis computation

An alternative method is to estimate the expansion coefficients using the following cost function:

$$\hat{c}_k = \operatorname*{argmin}_{c_k} \frac{1}{N} \sum_{n=0}^{N-1} \left| x[n] - \sum_{k=0}^{M-1} c_k \phi_k[n] \right|, \qquad (13)$$

which substitutes a mean of absolute errors for the mean of square errors used in the traditional Fourier analysis. Using the proposed Fourier analysis, the truncated Fourier expansion can approximate a function with a jump discontinuity with a more robust behavior against the amplitude changes at discontinuous points. We call this $\ell_1$ Fourier analysis or MAE Fourier analysis. Similarly, the traditional Fourier analysis is called $\ell_2$
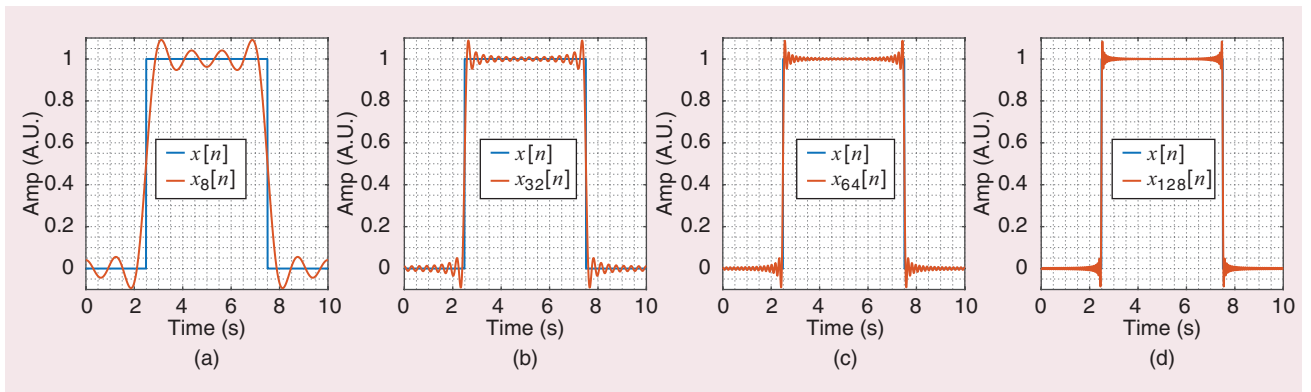


**FIGURE 1.** The result of the truncated Fourier expansion when the coefficients are computed using $\ell_2$ Fourier analysis ($x_M[n]$ for $M = 8, 32, 64,$ and 128) in approximating a step function with $N = 1,024$. (a) $M = 8$, (b) $M = 32$, (c) $M = 64$, and (d) $M = 128$.

Fourier analysis or MSE Fourier analysis as the coefficients are computed by minimizing the MSE. The optimization problem (13) is convex, but there is no analytic formula for its solution (i.e., it is difficult to minimize because the last term is nondifferentiable). However, it can be solved numerically in a linear computational complexity.

In this article, optimization problem (13) is solved using the MM approach [19]. The key idea of the MM approach is to convert the intractable original problem into a simpler one that can be solved. Specifically, the original cost function is approximated by an iterative tractable surrogate function. Then a solution is found by minimizing the surrogate function with nonincreasing cost. The obtained solution converges to a stationary point of the original optimization problem. To solve problem (13), we use a majorizer for the absolute value. That is,

$$|x[n]| \le \frac{1}{2} \frac{x^2[n]}{|x_M^{(r)}[n]|} + \frac{1}{2}|x_M^{(r)}[n]|, \quad (14)$$

with equality when $x[n] = x_M^{(r)}[n]$ ($x_M^{(r)}[n]$ is the estimated signal after $r$ iterations). In this case, (13) is expressed as

$$\hat{c}_k^{(r+1)} =$$
$$\underset{c_k}{\text{argmin}} \frac{1}{N} \sum_{n=0}^{N-1} \frac{\left(x[n] - \sum_{k=0}^{M-1} c_k \phi_k[n]\right)^2}{2|x[n] - x_M^{(r)}[n]|}$$
$$+ \frac{\gamma}{2}, \quad (15)$$

where $\gamma = |x[n] - x_M^{(r)}[n]|$ and

$$x_M^{(r)}[n] = \sum_{k=0}^{M-1} \hat{c}_k^{(r)} \phi_k[n].$$

The minimization of (15) with respect to the coefficients $c_k$ leads to the following solution:

$$\boldsymbol{c}_{\text{opt}}^{r+1} = (\boldsymbol{\Psi}^{(r)})^{-1} \tilde{\boldsymbol{x}}^{(r)} \quad (16)$$

where $\boldsymbol{\Psi}^{(r)} \in \mathbb{R}^{M \times M}$ and $\tilde{\boldsymbol{x}}^{(r)} \in \mathbb{R}^M$ are, respectively, matrices and vectors with the following entries:

$$\boldsymbol{\Psi}_{p,q}^{(r)} = \frac{1}{N} \sum_{n=0}^{N-1} \frac{\phi_p[n] \phi_q^*[n]}{|x[n] - x_M^{(r)}[n]|},$$
$$(p, q = 0, \dots, M-1)$$
$$\tilde{\boldsymbol{x}}_q^{(r)} = \frac{1}{N} \sum_{n=0}^{N-1} x[n] \frac{\phi_q^*[n]}{|x[n] - x_M^{(r)}[n]|}.$$
$$(17)$$

In this study, we consider the initial condition $x_M^{(0)}[n] = x[n] + \kappa$ where $\kappa$ is a nonzero constant value. In this case, the traditional approach (i.e., $\ell_2$ Fourier analysis) is a special case of $\ell_1$ Fourier analysis when $\kappa$ and the number of iterations, $r$, are both set to one ($\kappa = r = 1$). The proposed approach ($\ell_1$ Fourier analysis) was used to compute the coefficients of the truncated Fourier expansion of the step function in the previous example.

Figure 2 illustrates the performance of the truncated Fourier series with the first eight modes. The solid blue and red curves in Figure 2 denote the theoretical step function (i.e., $x[n]$) and its Fourier

expansion using $\ell_2$ Fourier analysis (i.e., $x_8[n]$), respectively, and are the same as those in Figure 1. The truncated Fourier expansion with the expansion coefficients obtained by $\ell_1$ Fourier analysis after $r = \{3, 5, 10, 50\}$ iterations (i.e., $x_8^{(r)}[n]$) is plotted in Figure 2 with a black solid line. The overshoot of the truncated Fourier expansion is reduced when the expansion coefficients are computed using $\ell_1$ Fourier analysis. Specifically, the overshoot is decreased as the number of iterations is increased. The cost function evolution of the MM approach is illustrated in Figure 3. It is seen that the algorithm converges well within a few iterations. In Figure 4(a) and (b), we illustrate the performance of the truncated Fourier series with the first 128 modes. The coefficients are computed by $\ell_1$ Fourier analysis after three and 10 iterations, respectively. The results show that the overshoot can be decreased to 4% of the magnitude of the jump.

Since the matrices $\boldsymbol{\Psi}^{(r)}$ in (16) are nonorthogonal, the $\ell_1$ Fourier analysis involves matrix inversion, which has a complexity of $O(M^3 + MN)$. There are three special spaces in convex optimization: 1) the $\ell_1$-norm, which mostly replaces the $\ell_0$-norm as the $\ell_0$-norm is not convex and not well defined, 2) the celebrated $\ell_2$-norm that everybody knows and uses, and 3) the $\ell_\infty$-norm. Other norm spaces mostly produce performances that are in between those of these spaces. We also employed the $\ell_\infty$-norm minimization to compute the Fourier analysis. The truncated Fourier
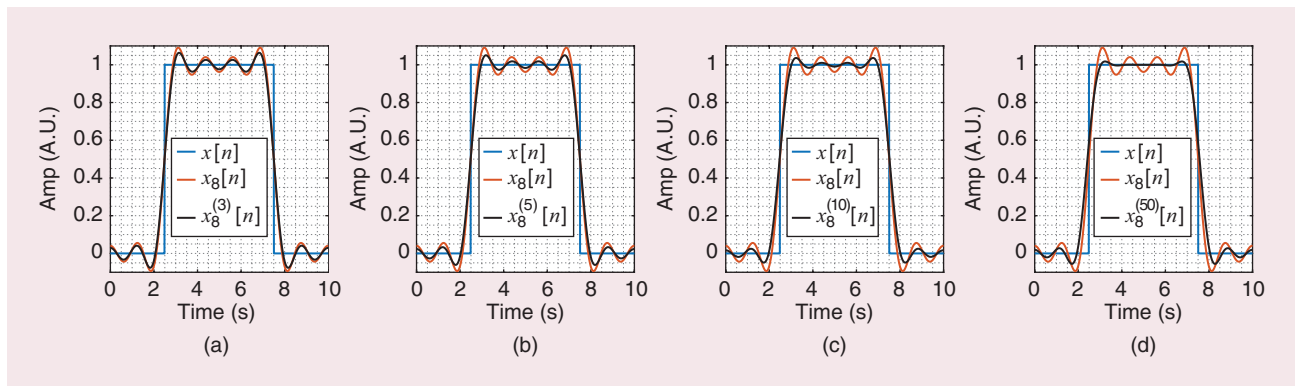


**FIGURE 2.** The result of the truncated Fourier expansion of $M = 8$ terms when the coefficients are computed using $\ell_1$ Fourier analysis after a certain iteration ($x_8^{(r)}[n], r = 3, 5, 10, 50$) in approximating the step function. (a) $r = 3$, (b) $r = 5$, (c) $r = 10$, and (d) $r = 50$.

expansion of the step function when the coefficients are computed using $\ell_\infty$ Fourier analysis is shown via the red color in Figure 5. The $\ell_8$- and $\ell_4$-norm minimizations are also employed to compute the Fourier analysis. The truncated Fourier expansion using $\ell_8$ and $\ell_4$ Fourier analyses are respectively shown via yellow and purple. As expected, these two norms produce a performance in between those of $\ell_1$- and $\ell_\infty$-norm minimization. In other words, the size of the overshoot/undershoot for truncated Fourier expansion decreases when we decrease the norm of minimization in a Fourier analysis computation.

## Applications

The new Fourier analysis can find various applications in signal processing. As a proof of concept, we focus on two examples.

### Reduction of the Gibbs phenomenon in image filtering

Signal decomposition-based methods, such as the Fourier transform, discrete cosine transform (DCT), and the wavelet transform, are common approaches to image filtering. In this section, we consider the DCT for low-pass filtering of an image. For a 2D signal $x[n_1, n_2]$, $n_1 = 0, 1, \ldots, N_1 - 1$, $n_2 = 0, 1, \ldots, N_2 - 1$, one possible 2D
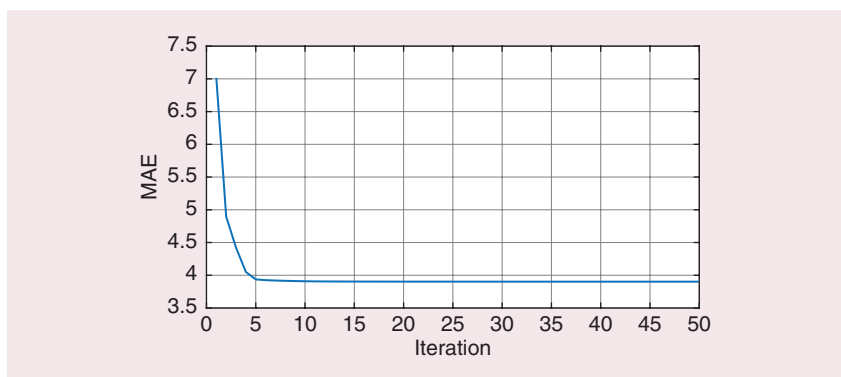
**FIGURE 3.** The convergence of the MM approach.

inverse discrete cosine transform (iDCT) is defined as

$$x[n_1, n_2] = \sum_{k_1=0}^{N_1-1} \sum_{k_2=0}^{N_2-1} c_{k_1,k_2} \phi_{k_1,k_2}[n_1, n_2],$$
(18)

where (19), listed in the box at the bottom of the page.

When we represent an image by an iDCT, the Gibbs phenomenon is the most common image artifact that arises from the truncated iDCT of the

image. For instance, consider the original image shown in Figure 6(a). We contaminated it with salt-and-pepper noise, as shown in Figure 6(b). Salt-and-pepper noise is an impulse noise that is sometimes seen on images. This noise can be caused by sharp and sudden disturbances in the image signal. We employed a truncated iDCT to reconstruct the original image, and the result is shown in Figure 6(c). The truncated iDCT is not a good model for reconstructing the

$$\begin{cases} \phi_{k_1,k_2}[n_1, n_2] = \cos \dfrac{k_1 \pi}{N_1}\left(n_1 + \dfrac{1}{2}\right) \cos \dfrac{k_2 \pi}{N_2}\left(n_2 + \dfrac{1}{2}\right) \\ c_{k_1,k_2} = \dfrac{1}{N_1 N_2} \sum_{n_1=0}^{N_1-1} \sum_{n_2=0}^{N_2-1} x[n_1, n_2] \phi_{k_1,k_2}[n_1, n_2] \end{cases}.$$
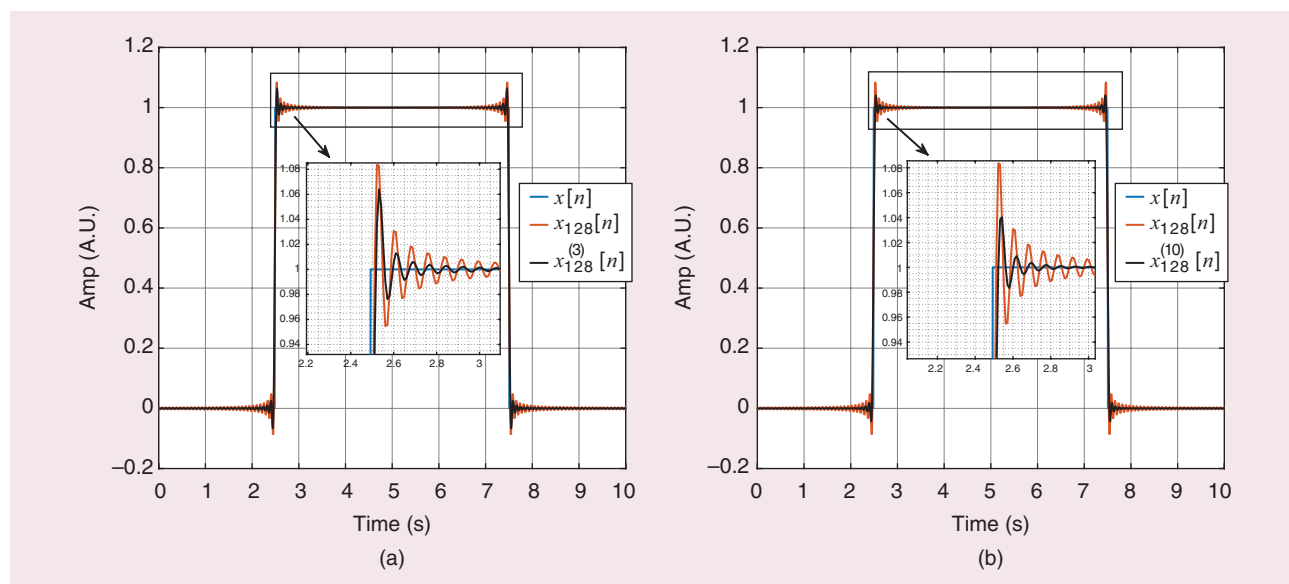(19)

**FIGURE 4.** The result of the proposed truncated Fourier expansion of $M = 128$ terms after a certain iteration, $x_8^{(r)}[n]$, in approximating the step function, for $r = 3, 10$. The truncated Fourier expansion using $\ell_2$ Fourier analysis ( $x_M[n]$ ) is also illustrated via the red line for comparison. (a) $r = 3$. (b) $r = 10$.

original image. The noise is not eliminated by the model, and the Gibbs effect is clear in the output. The weak performance of the truncated iDCT model is due to the approach used for the DCT computation. To show this, we computed the DCT using the $\ell_1$ optimization approach. The results of the truncated iDCT using the $\ell_1$ DCT after a certain iteration ($r = 2, 5, 15$) are shown in Figure 7. It is seen that the reconstructed image becomes close to the original image as the number of iterations increases. In other words, the Gibbs effect is reduced when $\ell_1$ optimization is used to compute the coefficients (i.e., the DCT). Therefore, the Gibbs effect is mainly due to the DCT computation approach but not the iDCT model. It is decreased in low-pass filtering of images while maintaining the sharp-edged features.

## Audio filtering

In this section, we compare the truncated Fourier expansion (when the coefficients are computed using $\ell_2$ or $\ell_1$ Fourier analysis) and a zero-phase Butterworth filter for denoising audio signals corrupted by random-valued impulse noise. For this purpose, we consider "guitartune.wav," the standard sample tune that ships with MATLAB. The signal contains 661,500 samples,
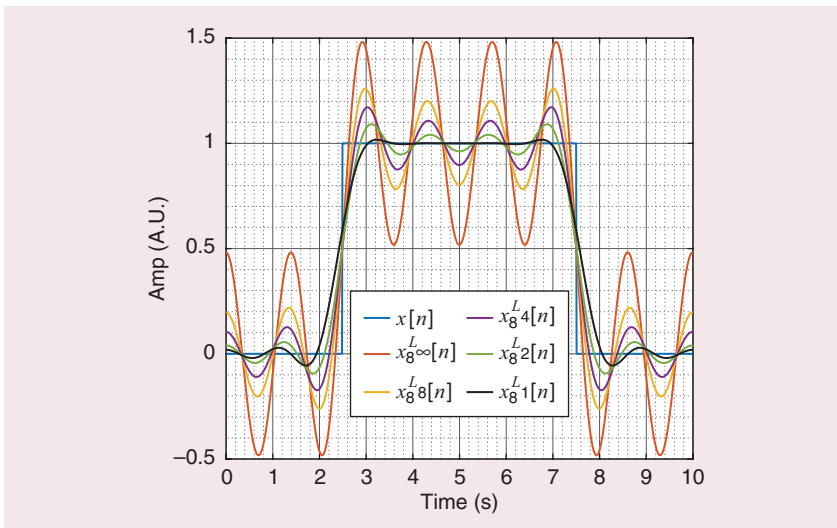


**FIGURE 5.** The result of the truncated Fourier expansion of $M = 8$ terms ($x_M^{\ell_p}[n]$) when the coefficients are computed using $\ell_\infty, \ell_8, \ell_4, \ell_2,$ and $\ell_1$ Fourier analyses in approximating the step function.
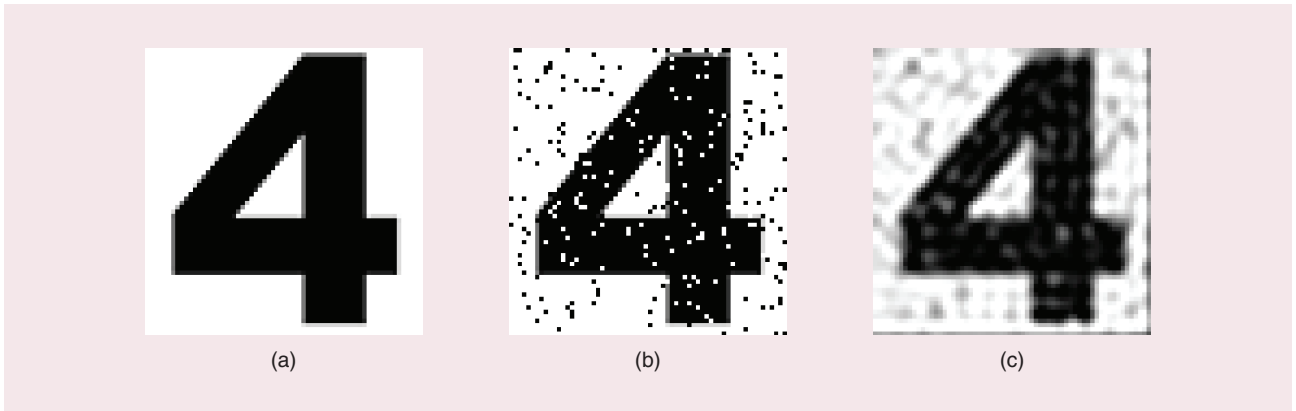


**FIGURE 6.** Image filtering using a truncated $\ell_2$ iDCT. (a) Original image, (b) noisy image obtained by adding salt-and-pepper noise, and (c) denoised image using the truncated $\ell_2$ iDCT.
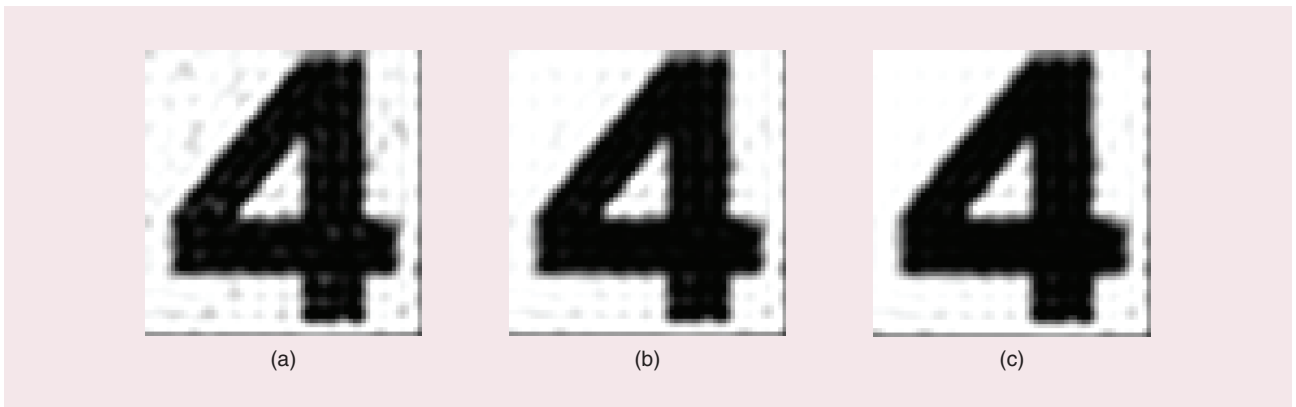


**FIGURE 7.** Image denoising using the truncated $\ell_1$ iDCT after a certain iteration, $r = 2, 5, 15$. (a) $r = 2$. (b) $r = 5$. (c) $r = 15$.
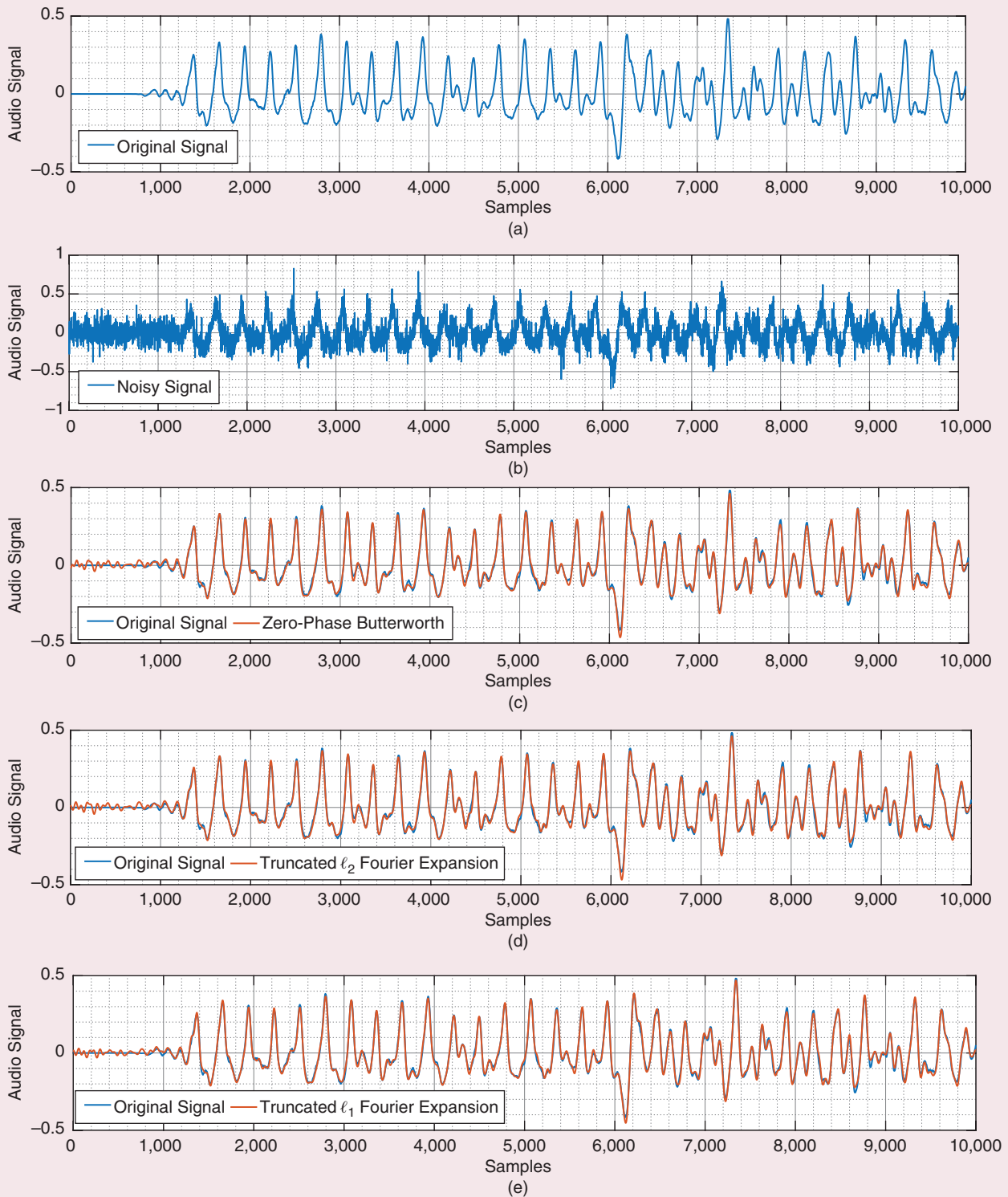
**FIGURE 8.** Audio filtering using zero-phase Butterworth filter (SRE = 0.1092 and ARE = 0.1152), truncated $\ell_2$ Fourier expansion (SRE = 0.1118 and ARE = 0.1183), and truncated $\ell_1$ Fourier expansion (SRE = 0.0963 and ARE = 0.1). (a) Original signal. (b) Noisy signal (SNR = 5 dB). (c) Zero-phase Butterworth filter. (d) Truncated $\ell_2$ Fourier expansion. (e) Truncated $\ell_1$ Fourier expansion. SRE: square relative error; ARE: absolute relative error.

which we split into subsignals, each containing 10,000 samples. Therefore, we have 66 signals. The signals were contaminated with impulse noise. For this purpose, we produced signals varying the power of noise. The signal-to-noise ratio (SNR) was modulated from –5 dB to 10 dB. The truncated Fourier expansion (using $\ell_2$ or $\ell_1$ Fourier analysis) and a third-order zero-phase Butterworth filter were then used to reconstruct the desired signals from the noisy signals. The cutoff frequency was set to 800 Hz. As an example, the first 10,000 samples of "guitartune. wav" and its noisy signal with SNR = 5 dB are shown in Figure 8(a) and (b), respectively. The results of audio signal filtering with these three methods are illustrated in Figure 8(c)–(e). For evaluating the performance of the methods, we used the average square relative error (SRE) and the average absolute relative error (ARE) of the estimation accuracy, defined by

$$SRE = \frac{\sum_k (x_k - \hat{x}_k)^2}{\sum_k x_k^2}$$

$$ARE = \frac{\sum_k |x_k - \hat{x}_k|}{\sum_k |x_k|}, \qquad (20)$$

where $x$ and $\hat{x}$ are the original and the estimated signal, respectively. The results of the reconstruction procedures using these metrics are reported in Figure 9(a) and (b). The SRE and ARE for the truncated Fourier expansion when the coefficients are computed using $\ell_1$ Fourier analysis are less than those of the zero-phase Butterworth filter and truncated Fourier expansion when the coefficients are computed using $\ell_2$ Fourier analysis, which means that the proposed $\ell_1$ Fourier expansion outperforms the other two methods.

## What we have learned
In a Fourier decomposition, the signal is represented as a linear combination of trigonometric or exponential basis functions, and the expansion weights (or coefficients) are computed such that they best fit the signal. In the traditional approach, the Fourier analysis (expansion coefficient) is computed based on the minimization of the MSE between the signal and its expansion (i.e., $\ell_2$-norm minimization of the error). In this approach, when a truncated Fourier expansion is used to approximate a signal with a jump discontinuity, an overshoot/undershoot at the discontinuity occurs, which is known as the Gibbs phenomenon. Using $\ell_2$ Fourier analysis, the size of the overshoot/undershoot is approximately 9% of the magnitude of the jump. We have learned that the size of the overshoot/undershoot is mainly due to the approach used for computing the Fourier analysis. The Fourier analysis can be computed using other $\ell_p$-norm minimizations. The size of the overshoot/undershoot changes if the Fourier analysis is computed based on the $\ell_p$-norm minimization of the model error. For $p \geq 1$, other $\ell_p$-norm minimizations mostly produce performances in between those of the $\ell_1$- and $\ell_\infty$-norm minimizations.

Some future directions are summarized as follows:

- Although different $\ell_p$-norm optimization approaches ($p \geq 1$) were used to compute the Fourier analysis, and $\ell_1$ Fourier analysis is the best choice for reducing the size of overshoot/undershoot in the truncated Fourier expansion of the step function, there are some improvements that can be done in the future.
- The extension of the proposed computing approach to $\ell_p$ Fourier analysis for $0 \leq p < 1$ is interesting. For instance, it would be interesting to see what the result would be by using $\ell_0$-norm minimization.
- The extension of the proposed method to compute the expansion coefficients of other signal decomposition-based methods, such as the wavelet transform, polynomial interpolation, and spline interpolation, is another possibility.
- Finally, $\ell_1$ Fourier analysis can be used to improve the accuracy of the Fourier expansion at the cost of increasing the computational complexity. Improving the computational complexity of the
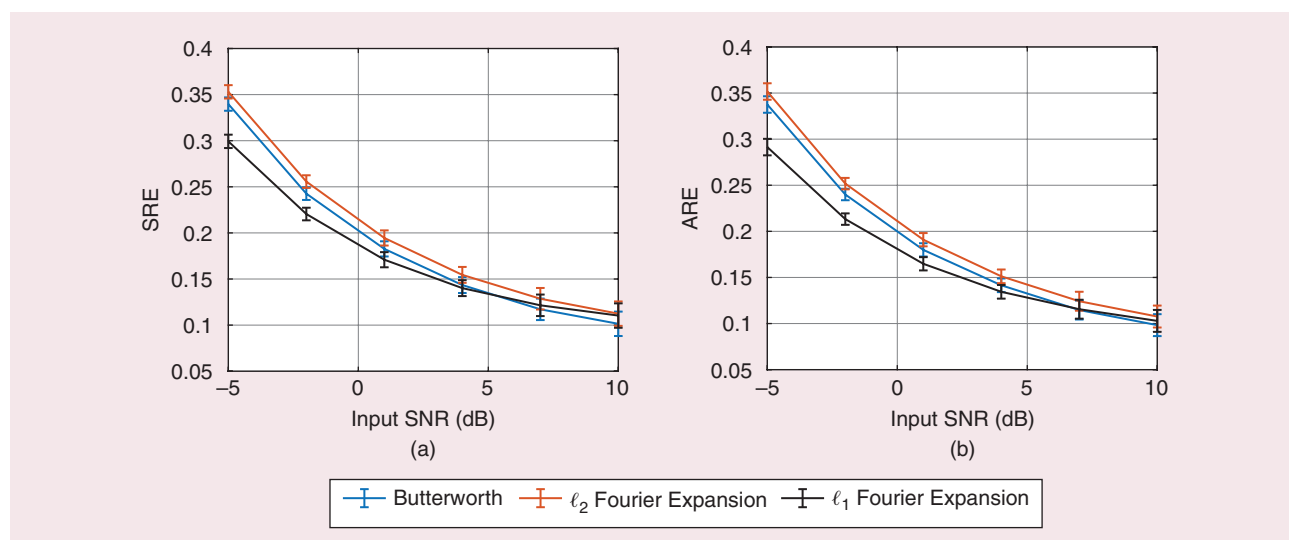


**FIGURE 9.** Audio low-pass filtering using $\ell_2$ and $\ell_1$ Fourier expansion and zero-phase Butterworth filter. (a) SRE. (b) ARE.

proposed approach can be considered as a topic of future work.

## Acknowledgment

## Author

*Arman Kheirati Roonizi* (ebad.kheirati.roonizi@gmail.com) received his Ph.D. degree in computer science from the University of Milan, Italy, in 2017. During 2017–2018, he held a postdoctoral research position with GIPSA-lab, Grenoble, France. He is currently an assistant professor in the Department of Computer Science, Fasa University, Fasa 74616-86131, Iran, and also a postdoctoral researcher with the Dipartimento di Informatica, Università degli Studi di Milano, 20131 Milano, Italy. His research interests include signal modeling, processing, filtering and separation, multimodal signal processing, sparsity, and functional data analysis. He is a Member of IEEE.

## References

[1] J. F. James, *A Student's Guide to Fourier Transforms: With Applications in Physics and Engineering*, 3rd ed. Cambridge, U.K.: Cambridge Univ. Press, 2011.

[2] K. R. Rao, D. N. Kim, and J.-J. Hwang, *Fast Fourier Transform - Algorithms and Applications*, 1st ed. Dordrecht, The Netherlands: Springer International Publishing, 2010.

[3] J. van der Hoeven, "The truncated Fourier transform and applications," in *Proc. 2004 Int. Symp. Symbolic Algebr. Comput. - ISSAC '04*, ACM Press, pp. 290–296, doi: 10.1145/1005285.1005327.

[4] E. S. Hewitt and R. E. Hewitt, "The Gibbs-Wilbraham phenomenon: An episode in Fourier analysis," *Arch. Hist. Exact Sci.*, vol. 21, no. 2, pp. 129–160, Jun. 1979, doi: 10.1007/BF00330404.

[5] W. Strauss, *Partial Differential Equations: An Introduction*. Hoboken, NJ, USA: Wiley, 2007.

[6] H.-G. Moon, "A low-complexity design for an MP3 multi-channel audio decoding system," *IEEE/ACM Trans. Audio, Speech, Lang. Process.*, vol. 20, no. 1, pp. 314–321, Jan. 2012, doi: 10.1109/TASL.2011.2161081.

[7] R. Baxter, "SAR image compression with the Gabor transform," *IEEE Trans. Geosci. Remote Sens.*, vol. 37, no. 1, pp. 574–588, Jan. 1999, doi: 10.1109/36.739117.

[8] D. K. Mynbaev and L. L. Scheiner, "Spectral analysis 2 – The Fourier transform in modern communications," in *Essentials of Modern Communications*. New York, NY, USA: Wiley, 2020, pp. 615–705.

[9] J. O. Smith, *Introduction to Digital Filters with Audio Applications*. W3K Publishing, 2007. [Online]. Available: http://www.w3k.org/books/

[10] J. R. I. Grattan-Guinness, *Joseph Fourier, 1768-1830: A Survey of His Life and Work*. Cambridge, MA, USA: MIT Press, 2003, p. 530.

[11] E. O. Brigham, *The Fast Fourier Transform*. Englewood Cliffs, NJ, USA: Prentice Hall, 1974.

[12] E. J. Candès, M. B. Wakin, and S. P. Boyd, "Enhancing sparsity by reweighted minimization," *J. Fourier Anal. Appl.*, vol. 14, nos. 5-6, pp. 877–905, Oct. 2008, doi: 10.1007/s00041-008-9045-x.

[13] A. Kheirati Roonizi, "$l_2$ and $l_1$ trend filtering: A Kalman filter approach [Lecture Notes]," *IEEE Signal Process. Mag.*, vol. 38, no. 6, pp. 137–145, Nov. 2021, doi: 10.1109/MSP.2021.3102900.

[14] E. J. Candès and M. B. Wakin, "An introduction to compressive sampling," *IEEE Signal Process. Mag.*, vol. 25, no. 2, pp. 21–30, Mar. 2008, doi: 10.1109/MSP.2007.914731.

[15] P. Schniter and S. Rangan, "Compressive phase retrieval via generalized approximate message passing," *IEEE Trans. Signal Process.*, vol. 63, no. 4, pp. 1043–1055, Feb. 2015, doi: 10.1109/TSP.2014.2386294.

[16] E. Candes, J. Romberg, and T. Tao, "Robust uncertainty principles: Exact signal reconstruction from highly incomplete frequency information," *IEEE Trans. Inf. Theory*, vol. 52, no. 2, pp. 489–509, Feb. 2006, doi: 10.1109/TIT.2005.862083.

[17] L. Gajny, O. Gibaru, and E. Nyiri, "L1 spline fits via sliding window process: Continuous and discrete cases," *Numer. Algorithms*, vol. 78, no. 2, pp. 449–464, Jul. 2017, doi: 10.1007/s11075-017-0383-0.

[18] P. Houston, S. Roggendorf, and K. G. Van Der Zee, "Gibbs phenomena for LQ-best approximation in finite element spaces," *ESAIM, Math. Model. Numer. Anal.*, vol. 56, no. 1, pp. 177–211, 2022, doi: 10.1051/m2an/2021086.

[19] Y. Sun, P. Babu, and D. P. Palomar, "Majorization-minimization algorithms in signal processing, communications, and machine learning," *IEEE Trans. Signal Process.*, vol. 65, no. 3, pp. 794–816, Feb. 2017, doi: 10.1109/TSP.2016.2601299.

[20] A. V. Oppenheim, R. W. Schafer, and J. R. Buck, *Discrete-Time Signal Processing*, 2nd ed. Englewood Cliffs, NJ, USA: Prentice Hall, 1999.

[21] D. E. Troncoso Romero and M. G. Cruz Jimenez, "Simplifying single-bin discrete Fourier transform computations [Tips & Tricks]," *IEEE Signal Process. Mag.*, vol. 38, no. 2, pp. 130–136, Mar. 2021, doi: 10.1109/MSP.2020.3046219.

[22] G. G. Kumar, S. K. Sahoo, and P. K. Meher, "50 years of FFT algorithms and applications," *Circuits Syst. Signal Process.*, vol. 38, no. 12, pp. 5665–5698, May 2019, doi: 10.1007/s00034-019-01136-8.

[23] L. Sujbert, G. Simon, and G. Peceli, "An observer-based adaptive Fourier analysis [Tips & Tricks]," *IEEE Signal Process. Mag.*, vol. 37, no. 4, pp. 134–143, Jul. 2020, doi: 10.1109/MSP.2020.2982167.

[24] A. A. Michelson, "Fourier's series," *Lett. Nature*, vol. 58, no. 1510, pp. 544–545, Oct. 1898, doi: 10.1038/058544b0.

[25] J. W. Gibbs, "Fourier's series," *Lett. Nature*, vol. 59, p. 200, Apr. 1899.

[26] J. W. Gibbs, "Fourier's series," *Lett. Nature*, vol. 59, p. 606, Apr. 1899.

[27] H. Wilbraham, "On a certain periodic function," *Cambridge Dublin Math. J.*, vol. 3, pp. 198–201, 1848. [Online]. Available: https://books.google.it/books?id=JrQ4AAAAMAAJ&pg=PA198&redir_esc=y#v=onepage&q&f=false

[28] S. E. Kelly, "Gibbs phenomenon for wavelets," *Appl. Comput. Harmon. Anal.*, vol. 3, no. 1, pp. 72–81, 1996, doi: 10.1006/acha.1996.0006.

SP